5-1-2018

Type 2 Diabetes Impairs the Ability of Skeletal Muscle Pericytes to Augment Postischemic Neovascularization in db/db Mice

Katherine L. Hayes
University of Massachusetts Amherst

Louis M. Messina
University of Massachusetts Chan Medical School

Lawrence M. Schwartz
University of Massachusetts Amherst

Jinglian Yan
University of Massachusetts Chan Medical School

Amy S. Burnside
University of Massachusetts Amherst

See next page for additional authors

Am J Physiol Cell Physiol 314: C534–C544, 2018.
First published January 10, 2018; doi:10.1152/ajpcell.00158.2017.

RESEARCH ARTICLE

Type 2 diabetes impairs the ability of skeletal muscle pericytes to augment postischemic neovascularization in *db/db* mice

Katherine L. Hayes,[1] Louis M. Messina,[2] Lawrence M. Schwartz,[3] Jinglian Yan,[2] Amy S. Burnside,[4] and Sarah Witkowski[1]

[1]*Department of Kinesiology, University of Massachusetts Amherst, Amherst, Massachusetts;* [2]*Diabetes Center of Excellence and Division of Vascular and Endovascular Surgery, University of Massachusetts Medical School, Worcester, Massachusetts;* [3]*Department of Biology, University of Massachusetts Amherst, Amherst, Massachusetts; and* [4]*Flow Cytometry Core Facility, Institute for Applied Life Sciences, University of Massachusetts Amherst, Amherst, Massachusetts*

Submitted 20 July 2017; accepted in final form 8 January 2018

Hayes KL, Messina LM, Schwartz LM, Yan J, Burnside AS, Witkowski S. Type 2 diabetes impairs the ability of skeletal muscle pericytes to augment postischemic neovascularization in *db/db* mice. *Am J Physiol Cell Physiol* 314: C534–C544, 2018. First published January 10, 2018; doi:10.1152/ajpcell.00158.2017.—Peripheral artery disease is an atherosclerotic occlusive disease that causes limb ischemia and has few effective noninterventional treatments. Stem cell therapy is promising, but concomitant diabetes may limit its effectiveness. We evaluated the therapeutic potential of skeletal muscle pericytes to augment postischemic neovascularization in wild-type and type 2 diabetic (T2DM) mice. Wild-type C57BL/6J and leptin receptor spontaneous mutation *db/db* T2DM mice underwent unilateral femoral artery excision to induce limb ischemia. Twenty-four hours after ischemia induction, $CD45^{-}CD34^{-}CD146^{+}$ skeletal muscle pericytes or vehicle controls were transplanted into ischemic hindlimb muscles. At postoperative day 28, pericyte transplantation augmented blood flow recovery in wild-type mice (79.3 ± 5% vs. 61.9 ± 5%; $P = 0.04$), but not in T2DM mice (48.6% vs. 46.3 ± 5%; $P = 0.51$). Pericyte transplantation augmented collateral artery enlargement in wild-type (26.7 ± 2 μm vs. 22.3 ± 1 μm, $P = 0.03$), but not T2DM mice (20.4 ± 1.4 μm vs. 18.5 ± 1.2 μm, $P = 0.14$). Pericyte incorporation into collateral arteries was higher in wild-type than in T2DM mice ($P = 0.002$). Unexpectedly, pericytes differentiated into Schwann cells in vivo. In vitro, Insulin increased *Nox2* expression and decreased tubular formation capacity in human pericytes. These insulin-induced effects were reversed by *N*-acetylcysteine antioxidant treatment. In conclusion, T2DM impairs the ability of pericytes to augment neovascularization via decreased collateral artery enlargement and impaired engraftment into collateral arteries, potentially via hyperinsulinemia-induced oxidant stress. While pericytes show promise as a unique form of stem cell therapy to increase postischemic neovascularization, characterizing the molecular mechanisms by which T2DM impairs their function is essential to achieve their therapeutic potential.

limb ischemia; pericytes; Schwann cells; type 2 diabetes

INTRODUCTION

Peripheral artery disease (PAD) is an atherosclerotic occlusive disease that most commonly manifests with limb ischemia. Although the prevalence of many cardiovascular diseases is on the decline, the prevalence of PAD has risen by ~24% worldwide from 2000 to 2010 and now affects over 200 million people (13, 22). The prevalence of type 2 diabetes (T2DM) is also increasing, and diabetes is the most powerful risk factor for the development of PAD. People with PAD experience pain, poor mobility, decreased quality of life, and increased risk of all-cause mortality. There are limited noninterventional pharmaceutical options for PAD patients with symptomatic disease. Thus, much hope exists for the development of an effective cellular therapy as an alternative to the existing invasive open surgical or catheter-based PAD treatment paradigms.

Pericytes are a novel therapeutic target for a PAD cell therapy, and they have distinct advantages as a therapeutic strategy for the treatment of symptomatic PAD. Pericytes are located in a periendothelial position along the microvasculature, including precapillary arterioles, capillaries, and postcapillary venules. They are tissue resident cells that are crucial for angiogenesis via interactions with endothelial cells (14, 24). They may also be advantageous during postischemic neovascularization through differentiation into multiple terminally differentiated cells (1, 24), including skeletal myocytes (4, 5, 9) and endothelial cells (16). These advantages, especially their multipotent differentiation potential, provide a mechanism by which they might restore blood flow to an ischemic tissue. However, T2DM may impair pericyte function. Thus, before they can be exploited for a cellular therapy to treat PAD, the effect of diabetes on pericyte function during postischemic neovascularization must be evaluated.

Diabetes and PAD often occur together; furthermore, the natural course of PAD is worse in diabetics (27). This is important because diabetes has been shown to diminish the therapeutic potential of stem cells for the treatment of PAD (30). Evidence suggests that mesenchymal stem cells (MSCs) have diminished capacity to promote postischemic neovascularization in T2DM mice via diabetes-induced oxidant stress (30). The reduced function of MSCs in diabetic mice was shown to be due in part to altered differentiation capacity (30). However, no studies to date have evaluated skeletal muscle pericytes as a therapeutic strategy to treat PAD in diabetics.

Address for reprint requests and other correspondence: K. Hayes, UMass Medical School, AC7-2004, 368 Plantation St., Worcester, MA 01605 (e-mail: katherine.hayes@umassmed.edu).

Table 1. *Antibodies*

Antibody	Conjugate	Use	Vendor
CD45	PE	FACS	BD Biosciences
CD34	BV421	FACS/characterization	BD Biosciences
CD146	Alexa Fluor 647	FACS/characterization	BD Biosciences
CD31		ICC	Abcam
Osteopontin		ICC	R&D Systems
MHC		ICC	DSHB
CD45	BUV395	Characterization	BD Biosciences
CD73	PE	Characterization	BD Biosciences
CD90	PE	Characterization	BD Biosciences
CD105	PE	Characterization	BD Biosciences
PDGFRβ	PE	Characterization	Abcam
CD144	PE	Characterization	BD Biosciences
CD144		IHC	BD Biosciences
αSMA		IHC	Thermo Fisher
GFP		IHC	Abcam
S100	FITC	IHC	Abcam

CD, cluster of differentiation; MHC, myosin heavy chain; PDGFRβ, platelet-derived growth factor receptor-β; αSMA, α-smooth muscle actin; GFP, green fluorescent protein; FACS, fluorescence-activated cell sorting; ICC, immunocytochemistry; IHC, immunohistochemistry; DSHB, Developmental Studies Hybridoma Bank.

The purpose of this study was to determine the effect of pericyte cell therapy on postischemic neovascularization after induction of hindlimb ischemia in wild-type and T2DM mice. We tested the central hypothesis that T2DM impairs the ability of skeletal muscle-derived pericytes to augment postischemic neovascularization after induction of hindlimb ischemia via impaired vascular remodeling and in vivo differentiation.

METHODS

Antibodies and reagents. Antibodies were obtained as indicated in Table 1. Reagents were obtained as follows: MEM alpha, RNAqueous-Micro Kit, and Superscript III First-Strand Synthesis SuperMix from Thermo Fisher Scientific; hydrocortisone, MesenCult Basal Medium with Adipogenic Stimulatory Supplements, and VEGF from STEMCELL Technologies; StemXVivo Base Medium with Osteogenic Supplements from R&D Systems; and Kapa SYBR FAST qPCR kit from Kapa Biosystems; Retrieve-All Antigen Unmasking System 2 (Basic pH 10) from BioLegend.

Animals. Three-month-old, male wild-type (C57BL/6J, Jackson Laboratories; $n = 12$) and leptin receptor mutation *db/db* T2DM mice (B6.Cg-*m* +/+ Lepr^{db}/J mice, Jackson Laboratories; $n = 10$) underwent induction of limb ischemia and were the recipient mice for pericyte cell transplant or vehicle control transplant. Mice that ubiquitously express enhanced green fluorescent protein (GFP) under the direction of the human ubiquitin C promotor [C57BL/6-Tg(UBC-GFP)30Scha/J; Jackson Laboratories, Bar Harbor, ME] were the donor mice for pericyte isolation and transplantations. All mice were fed ad libitum using a standard chow that contains 5.7% fat by weight. The Institutional Care and Use Committee of the University of Massachusetts Medical School approved all animal protocols.

Pericyte characterization. Thigh, gastrocnemius, and tibialis anterior muscles were dissected, minced, digested with collagenases (100 mg/ml) for 1.5 h at 37°C, then serially filtered through 100 μm, 70 μm, and 40 μm nylon meshes. Cell suspensions were incubated with anti-mouse CD16/CD32 (1 μg/million cells) for 15 min to block nonspecific Fc-mediated interactions. Next, cells were stained at 1:100 in 2% FBS in Dulbecco's PBS at 4°C for 20 min with antibodies against CD45, CD34, CD146, and an additional phycoerythrin (PE)-conjugated antibody against either CD73, CD90, CD105, platelet-derived growth factor receptor-β (PDGFRβ), CD144, or the appropriate IgG control. Flow cytometry was performed on a BD Dual LSRFortessa (BD Biosciences). Gates were established using fluorescence minus one controls; compensation was performed. Single cells were selected based on physical parameters, such as forward and side scatter area, height, and width; doublet discrimination was performed. We gated for $CD45^-CD34^-CD146^+$ pericytes based on previous research that showed this population was enriched for pericytes in human skeletal muscle (6, 7, 21). The percentage of PE^+ $CD45^-CD34^-CD146^+$ cells was determined for each surface marker.

Fluorescence-activated cell sorting (FACS) was used to sort for $CD45^-CD34^-CD146^+$ pericytes for gene expression analysis and in vitro differentiation assays. Skeletal muscles were dissected, minced, digested, and stained with antibodies against CD45, CD34, and CD146 as described above. Sorting yielded ~1–2% $CD45^-CD34^-CD146^+$ pericytes from whole skeletal muscle, and sorting efficiency ranged from 70 to 90%.

Immediately after sorting, an RNAqueous-Micro Kit was used to isolate RNA from 2×10^5 $CD45^-CD34^-CD146^+$ pericytes and an equal number of control cells (unsorted skeletal muscle cells that had been isolated and treated in the same manner as the pericytes). RNA concentration was determined via NanoDrop Spectrophotometry. cDNA synthesis was performed using Superscript III First-Strand Synthesis SuperMix with 100 ng of RNA. Kapa SYBR FAST qPCR was used to perform qRT-PCR using 1.5 μl of cDNA template. Reactions were run in triplicate. The average cycle threshold (C_t) was used for data analysis. Differences in relative gene expression were determined using the $\Delta\Delta C_t$ method. *BestKeeper* Excel-based tool, which utilizes pairwise correlations to determine a stably expressed housekeeping gene (20), was used to create an index of most suitable reference genes from five potential genes [eukaryotic elongation factor 2 (*Eef2*), aryl-hydrocarbon receptor-interacting protein (*Aip*), ribosomal protein L38 (*Rpl38*), CXXC-type zinc finger protein 1 (*Cxxc1*), and β-actin (*Bact*)]. As a result of the *BestKeeper* analysis, the C_t values for *Cxxc1* and *Eef2* were averaged and used as the reference C_t value. Primer sequences are presented in Table 2.

To perform in vitro differentiation assays, sorted $CD45^-CD34^-CD146^+$ pericytes were seeded on 0.2% gelatin in MEM alpha supplemented with 12.5% FBS, 10^{-4} M 2-mercaptoethanol, 10^{-5} M hydrocortisone, and 1% penicillin-streptomycin. At 80–90% confluence, pericytes were split 1:1 on polystyrene tissue culture plates. *Passage 2* cells were seeded in 8-well chamber slides for

Table 2. *Primers used for qRT-PCR*

Gene	Forward Primer (5′–3′)	Reverse Primer (3′–5′)
Pax3	AGTGCAGGTCTGGTTTAGCA	GGTCTCCGACAGCTGGTAT
Pax7	CTCCTCAGGTCATGAGCATCC	GTGGGCAGTAAGACTGGGAC
Cd31	GTCATGGCCATGGTCGAGTA	TCCTCGGCGATCTTGCTGAA
Sca1	TTCTCTGAGGATGGACACTTCT	GGTCTGCAGGAGGACTGAGC
MyoD	GCTACCCAAGGTGGAGATCCT	GGCGGTGTCGTAGCCATT
Eef2	CTGGTGGAGATCCAGTGTCC	GCCTTGACCACAAACATGGG
Rpl38	GTTCTCATCGCTGTGAGTGT	TTGACAGACTTGGCATCCTTCC
Aip	GCTCCGTTATAGATGACAGC	ATCTCGATGTGGAAGATGAG
Bact	CCTCTATGCCAACACAGTGC	CATCGTACTCCTGCTTGCTG
Cxxc1	CAGACGTCTTTTGGGTCCA	AGACCTCATCAGCTGGCAC
18s	CGGCTACCACATCCACGGAA	GCTGGAATTACCGCGGCT
Nox1	CAGCAGAAGGTCGTGATTACCAAG	AACTGTATGCTGATCCTGCTGC
Nox2	GTTCTCATTGTCACCGATGTCAG	GTTCTCATTGTCACCGATGTCAG
Nox4	TGTTGGGCCTAGGATTGTGTT	AGGGACCTTCTGTGATCCTCG

Pax3, paired box 3; *Pax7*, paired box 7; *Cd31*, cluster of differentiation 31; *Sca1*, stem cell antigen 1; *MyoD*, myogenic differentiation; *Eef2*, eukaryotic elongation factor 2; *Rpl38*, ribosomal protein L38; *Aip*, aryl-hydrocarbon receptor-interacting protein; *Cxxc1*, CXXC-type zinc finger protein 1; Bact, β-actin; *Nox1*, NADPH oxidase 1; *Nox2*, NADPH oxidase 2; *Nox4*, NADPH oxidase 4; *18s*, 18s ribosomal RNA.

24 h in growth medium, then the medium was changed to a selective differentiation medium, as follows: for adipocytes, MesenCult Basal Medium with Adipogenic Stimulatory Supplements for 21 days (30); for endothelial cells, Mesencult Basal Medium with 50 ng/ml VEGF for 7 days (30); for osteocytes, StemXVivo Base Medium with Osteogenic Supplements for 28 days (30); for muscle, muscle proliferation medium containing DMEM high-glucose supplemented with 10% FBS, 10% horse serum, 1% chick embryo extract for 7 days followed by lowering the serum concentration from 20% to 2% by replenishing half the medium every 3 days over 7–10 days with myogenic (muscle fusion) medium containing DMEM high-glucose supplemented with 1% FBS, 1% horse serum, and 0.5% chick embryo extract (5).

To visualize differentiation, immunocytochemistry was performed as follows: for endothelial cell differentiation, cells were stained with anti-CD31 antibody (1:20) for 90 min at 37°C, and then stained with goat anti-rabbit antibody (1:100) for 45 min at 37°C; for osteogenesis, cells were stained with anti-osteopontin antibody at 10 μg/ml at 4°C overnight, and then incubated with Alexa 488-conjugated donkey anti-goat antibody at 1:200 for 1 h; for muscle differentiation, cells were stained with anti-myosin heavy chain (MHC) antibody at 5 μg/ml for 90 min at 37°C, and then stained with goat anti-mouse Dylight 549 antibody at 1:100 for 1 h. The above cells were stained with DAPI before mounting and imaging. For adipogenesis, cells were washed with 60% isopropanol for 5 min, dried completely, incubated with Oil Red O working solution, then thoroughly washed before imaging.

Hindlimb ischemia and blood flow recovery assessment. Unilateral femoral artery ligation and excision under 1–2% isoflurane was used to induce hindlimb ischemia (19, 25, 26, 29). For pain relief, the analgesic buprenorphine was administered subcutaneously presurgery, 4 h postsurgery, and as needed for 48 h at 0.1 mg/kg; the analgesic ketoprofen was administered subcutaneously presurgery and 24 h postsurgery at 5 mg/kg. Blood flow in both hindlimb feet was simultaneously assessed noninvasively presurgery, immediately postsurgery, and then on postoperative days (POD) 3, 7, 14, 21, and 28 via laser Doppler perfusion imaging (LDPI; Moor Instruments, Devon, UK). Three repeated trials of flow data were collected and averaged. Data are expressed as a ratio of ischemic versus nonischemic hindfoot.

Pericyte transplantation. One-day postinduction of limb ischemia, 1×10^5 pericytes were sorted from GFP^+ donor mice. Cells were pooled from multiple donor mice to limit variability. Sorted pericytes were immediately transplanted into wild-type ($n = 6$) and T2DM mice ($n = 5$). Control wild-type ($n = 6$) and control T2DM mice ($n = 5$) were injected with an equal volume of vehicle control (150 μl sterile PBS). Injections were done under 1–2% isoflurane anesthesia intramuscularly into ischemic hindlimbs at three sites in the thigh region and two sites in the gastrocnemius (30 μl/site). Animals were randomly assigned into the pericyte transplantation or control groups. Control and experimental procedures were done side by side in age-matched animals. Equal numbers of animals from each group were housed together to ensure similar handling.

Angiogenesis and collateral artery enlargement. Ischemic gastrocnemius and thigh muscles were dissected at 28 days postinduction of hindlimb ischemia and then frozen at −80°C in OCT. Muscles were sectioned to 10 μm for immunohistochemistry analysis. In gastrocnemius, capillaries were stained with an antibody against CD144 (1:40, 4°C overnight) followed by staining with Alexa 594-conjugated goat anti-rat IgG (1:100 for 2 h). Sections were DAPI mounted, and five random images per muscle section were taken. Capillary-to-fiber ratio (number of $CD144^+$ capillaries per number of muscle fibers) and capillary density (number of $CD144^+$ capillaries per muscle fiber area) were quantified by two blinded observers; counts from both observers were averaged for data analysis. Muscle fiber area was assessed in Adobe Photoshop (Adobe Photoshop CC 2015) using the magnetic lasso tool to trace muscle fibers.

To detect collateral arteries, thigh cryosections were stained with anti-CD144 antibody (1:40, 4°C overnight) followed by staining with Alexa 594-conjugated goat anti-rat IgG (1:100 for 2 h); and then sequentially stained with anti-α-smooth muscle actin (αSMA; 1:2 at 4°C overnight) followed by staining with Dylight 488-conjugated goat anti-mouse subclass 2a (1:100 for 2 h). Sections were DAPI mounted and all cross-sectional collateral arteries were imaged. Images were analyzed by a blinded observer using Adobe Photoshop. Since compression artifacts can confound diameter measurements, the perimeter of the inner collateral artery wall was measured using the magnetic lasso tool, and then perimeter was converted to diameter (18).

In vivo pericyte differentiation. Immunohistochemistry was used to investigate costaining of GFP and phenotypic markers of terminal cell types. Gastrocnemius and thigh muscles from mice that were transplanted with pericytes were cryosectioned at 8 μm onto slides preheated to 45°C. Sections were immediately fixed in 37% paraformaldehyde at 45°C. Antigen retrieval was performed with Retrieve-All Antigen Unmasking System 2. Sections were incubated with anti-GFP antibody at 10 μg/ml in blocking solution overnight at 4°C followed by incubation with Alexa Fluor 568 donkey anti-goat IgG secondary antibody at 10 μg/ml in PBS for 2 h. To confirm GFP antibody specificity, the following controls were used: a wild-type tissue negative control, an IgG negative control, and a GFP positive control. Following anti-GFP labeling, sections were sequentially labeled with antibodies to visualize either endothelial cells, collateral arteries, or Schwann cells, as follows: for endothelial cells, anti-CD144 (1:40, 4°C overnight) followed by staining with Alexa 594-conjugated goat anti-rat IgG (1:100 for 2 h), for smooth muscle cells, anti-αSMA (1:2, 4°C overnight) followed by staining with Dylight 488-conjugated goat anti-mouse (1:100 for 2 h); for Schwann cells, FITC-conjugated anti-s100 antibody (1:50, 2 h at room temperature). All sections were DAPI mounted. A Nikon A1 Spectral Detector Confocal microscope was used to scan the tissues at ×20 for instances of GFP and phenotypic marker costaining. High-magnification (×600) images were acquired to confirm costaining. Images were taken of all αSMA collateral arteries, and the percentage of GFP^+ collateral arteries was quantified.

In vitro human primary pericyte oxidative stress and tube formation capacity. To determine if type 2 diabetes induces oxidant stress that impairs pericyte function in vitro, human primary pericytes that were isolated from placental tissue were purchased from PromoCell (Heidelberg, Germany). According to the supplier, over 98% of pericytes are positive for CD146. Pericytes were maintained in culture in DMEM with 10% FBS and 1% penicillin-streptomycin. To examine if hyperinsulinemia induces oxidative stress, 174 nM insulin (30) was added to the culture medium for 48 h. To examine if an antioxidant can prevent insulin-induced oxidative stress, 174 nM insulin plus 100 μM *N*-acetylcysteine (NAC) was added to cultures for 48 h. RNA was isolated from three replicates each of untreated controls, insulin treated, and insulin plus NAC-treated pericytes to quantify gene expression of NADPH oxidases (*Nox1*, *Nox2*, and *Nox4*) using qRT-PCR (primers shown in Table 2). Five replicates each of control and treated pericytes were plated in a 96-well plate on growth factor reduced matrigel in serum-free medium to induce tube formation. After 9 h, images of each entire well were taken. All of the tubular structures and characteristics in each well were quantified using the Angiogenesis Analyzer plugin for ImageJ. Total tube length represents the total length of all segments, including all segments and branches. Tube area is the average area of enclosed tubular structures. Master junctions link multiple branching segments and indicate the complexity of the tubular network.

Statistical analysis. Results are expressed as means ± SE. Linear mixed models (fixed effects: time and transplant group; random effect: mouse) were used to determine differences in blood flow

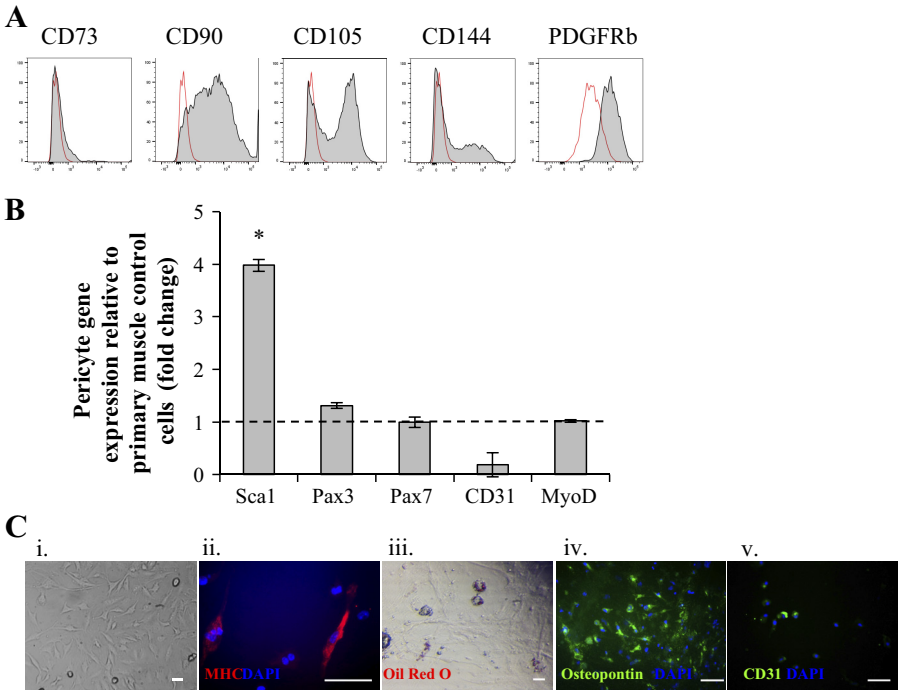

Fig. 1. Cell surface marker expression, gene expression, and in vitro differentiation of CD45$^-$CD34$^-$CD146$^+$ skeletal muscle pericytes. *A*: cell surface marker expression for mesenchymal stem cell (CD73, CD90, and CD105), endothelial (CD144), and pericyte (PDGFRβ) markers. *B*: gene expression in pericytes relative to gene expression in muscle tissue homogenate (dashed line) for stem cell antigen-1 (*Sca1*), paired box 3 (*Pax3*), paired box 7 (*Pax7*), *CD31*, and myogenic differentiation 1 (*MyoD*). *C*: in vitro differentiation of CD45$^-$CD34$^-$CD146$^+$ pericytes into skeletal muscle (*ii*), adipocytes (*iii*), osteocytes (*iv*), endothelial cells (*v*), and undifferentiated cells (*i*). Scale bar, 100 μm. *$P < 0.05$ vs. control.

recovery over time between experimental and control transplantation groups. Tukey's post hoc testing was used to determine differences between control and experimental groups at each time point. Student's *t*-tests were used to test for differences in capillary-to-fiber ratio, capillary density, and collateral diameter between experimental and control groups. Student's *t*-tests were used to test for differences in GFP$^+$ pericyte engraftment between wild-type and T2DM groups. One-way ANOVA for parametric data or Kruskal-Wallis one-way ANOVA for nonparametric data was used to test for differences in tube formation parameters between groups followed by Tukey's post hoc testing or multiple pairwise comparisons with Bonferroni corrections. Significance was accepted at an α-level of $P \leq 0.05$.

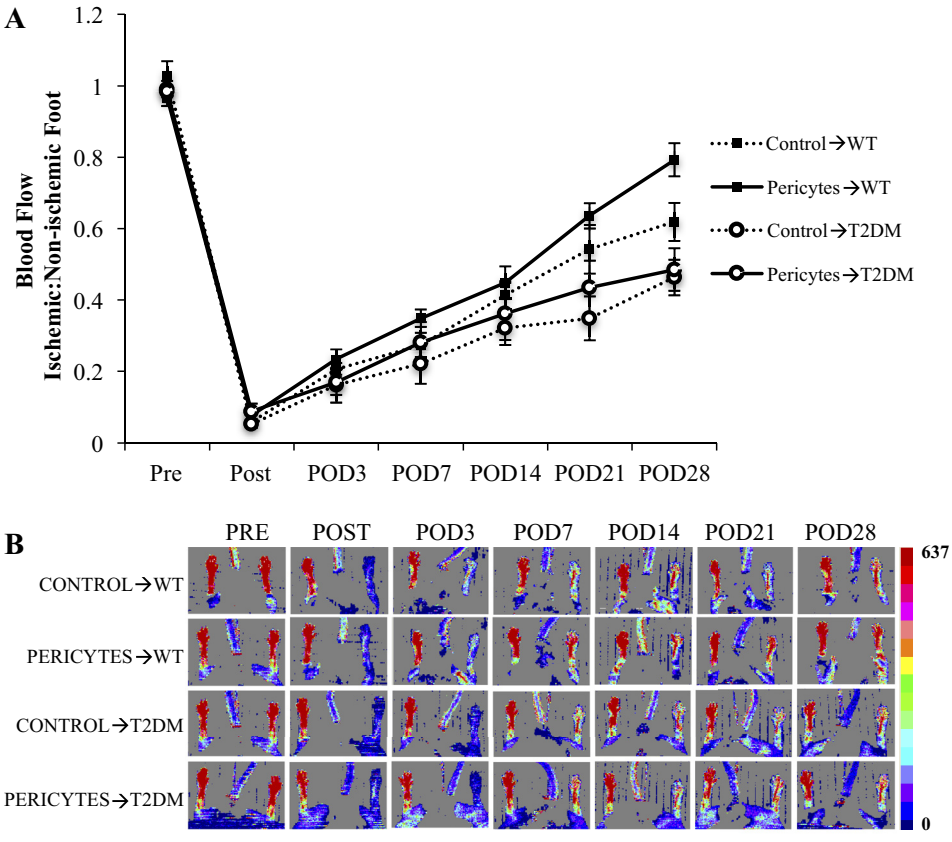

Fig. 2. Blood flow recovery from hindlimb ischemia in wild-type (WT) and type 2 diabetes mellitus *db/db* (T2DM) recipient mice. *A*: foot blood flow recovery assessed by laser Doppler perfusion imaging (LDPI). Values are means ± SE, $n = 6$ per group for WT, $n = 5$ per group for T2DM. *$P < 0.05$ for Pericyte→WT vs. Control→WT. *B*: representative LDPI images at each time point. POD, postoperative day; "→" indicates "transplanted into."

RESULTS

$CD45^-CD34^-CD146^+$ skeletal muscle cells are predominately pericytes. $CD45^-CD34^-CD146^+$ cells were predominately positive for CD105 (65%) and CD90 (74%), which are surface markers expressed by both pericytes and mesenchymal stem cells (MSCs); cells were also positive for the pericyte marker PDGFRβ (42%) in addition to being sorted on the pericyte marker CD146. Cells were weakly positive for the endothelial cell marker, CD144 (36%), and mostly negative for the MSC marker CD73 (7.9%) (Fig. 1*A*).

Gene expression data further confirmed the pericyte phenotype (Fig. 1*B*). There was significantly greater stem cell antigen-1 (*Sca-1*) gene expression in $CD45^-CD34^-CD146^+$ pericytes than in the whole muscle tissue homogenate (4.0-fold; $P < 0.01$). There was significantly lower CD31 gene expression in $CD45^-CD34^-CD146^+$ pericytes than in the whole muscle tissue homogenate (0.2-fold, $P < 0.01$). There was no difference in *Pax3*, *Pax7*, or *MyoD* gene expression in the sorted $CD45^-CD34^-CD146^+$ pericytes than in the whole muscle tissue homogenate (*Pax3*: 1.3-fold, *Pax7*: 1.0-fold, and *MyoD*: 1.0-fold, respectively; $P > 0.05$).

Pericytes are also defined by their ability to differentiate into mesodermal cell lineages. $CD45^-CD34^-CD146^+$ pericytes differentiated in vitro into muscle cells, adipocytes, osteocytes, and endothelial cells (Fig. 1*C*). In myogenic differentiation medium, pericytes differentiated into elongated, multinucleated cells that were positive for myosin heavy chain (MHC). In adipogenic medium, pericytes differentiated into adipocytes that stained positive for Oil Red O. In osteogenic differentiation medium, pericytes differentiated into cells that stained positive for osteopontin. In endothelial cell differentiation medium, cells expressed the endothelial cell marker CD31. Taken together, surface marker expression, gene expression, and in vitro differentiation potential indicate that the majority of $CD45^-CD34^-CD146^+$ cells are pericytes.

Pericyte transplantation augments blood flow recovery in wild-type, but not T2DM hindlimb ischemic mice. In wild-type mice, there was a significant main effect of pericyte transplantation ($P = 0.03$). There was a trend toward a time × transplantation interaction ($P = 0.09$), whereby at POD 28, wild-type mice that were transplanted with pericytes had significantly higher blood flow recovery than those that received the vehicle control (79.3 ± 5 vs. 61.9 ± 5%; $P = 0.04$) (Fig. 2).

T2DM mice had significantly lower blood flow recovery than wild-type mice after the induction of limb ischemia ($P < 0.001$). Overall in T2DM mice, there was no main effect of pericyte transplantation ($P = 0.51$) and no time × transplan-

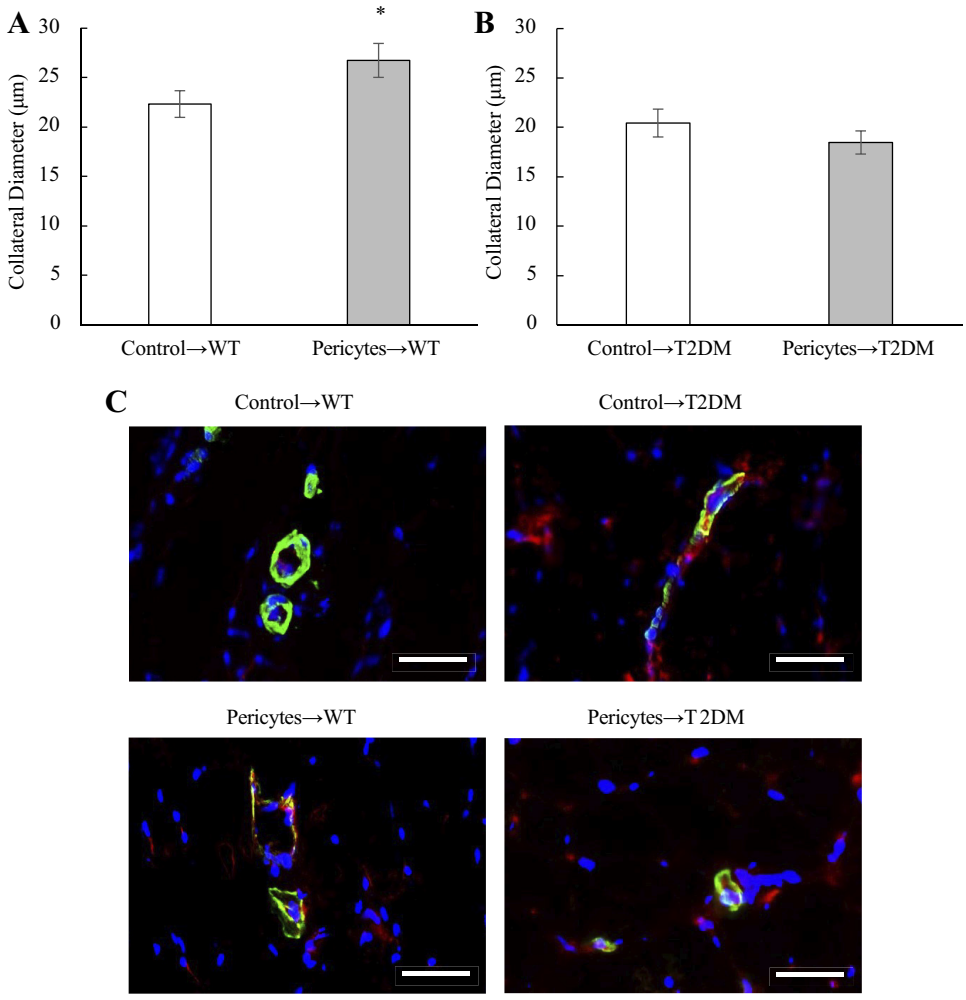

Fig. 3. Quantification of collateral artery diameter in wild-type (WT) and type 2 diabetes mellitus *db/db* (T2DM) ischemic mice. Collateral artery diameter was assessed in thigh muscle of WT mice (means ± SE, $n = 6$, $^*P = 0.03$ vs. Control→WT) (*A*) and T2DM (means ± SE, $n = 5$) (*B*) at POD28 following the induction of limb ischemia. Representative images (*C*) of CD144 (red) and α-smooth muscle actin (αSMA; green) double-staining of collateral arteries (DAPI in blue). Scale bars, 50 μm.

tation interaction ($P = 0.96$). At POD 28, T2DM that were transplanted with pericytes had similar blood flow recovery as those that received the vehicle control (48.6 ± 6% vs. 46.3 ± 5%) (Fig. 2).

Pericyte transplantation augments collateral artery enlargement in wild-type, but not T2DM hindlimb ischemic mice. In wild-type mice, the average collateral artery diameter was 17.9% greater in mice that were transplanted with pericytes than in mice transplanted with vehicle control (26.7 ± 2 μm vs. 22.3 ± 1 μm, $P = 0.03$; Fig. 3*A*). In T2DM mice, the average collateral artery diameter was not significantly different between mice transplanted with pericytes or vehicle control (9.7% difference; 20.4 ± 1.4 μm vs. 18.5 ± 1.2 μm, $P = 0.14$; Fig. 3*B*).

Pericyte transplantation does not improve angiogenesis. In wild-type mice, pericyte transplantation failed to increase capillary density (508.3 ± 66 vs. 453.2 ± 34 capillary/mm^2 in control, $P = 0.16$; Fig. 4*A*) and capillary-to-fiber ratio (1.18 ± 0.04 vs. 1.26 ± 0.06 in control, $P = 0.23$; Fig. 4*C*). In T2DM mice, pericyte transplantation also failed to increase capillary density (550.7 ± 47 vs. 569.8 ± 105 capillary/mm^2 in control, $P = 0.46$; Fig. 4*B*) and capillary-to-fiber ratio (0.99 ± 0.07 vs. 1.00 ± 0.05 in control, $P = 0.44$; Fig. 4*D*).

Transplanted pericytes incorporate into host vasculature and nerves, but not skeletal muscle in vivo. In both wild-type and T2DM mice, instances of the endothelial cell marker CD144 and GFP double staining were observed in collateral arteries (Fig. 5*A*). To confirm that GFP$^+$ pericytes were incorporating into collateral arteries, skeletal muscles were examined for instances of double-positive GFP and αSMA collateral arteries (Fig. 5*B*). There was a significantly greater percentage of αSMA$^+$ collateral arteries that costained positive for GFP in wild-type mice than in T2DM mice (25.0 ± 1% vs. 11.3 ± 3%, respectively; $P = 0.002$; Fig. 5*C*).

GFP$^+$ cells were also observed near collateral arteries. Morphology suggested that these positive cells were neural in origin, possibly Schwann cells. To investigate if GFP$^+$ pericytes differentiated into Schwann cells, skeletal muscle sections were examined for double-staining of GFP and the Schwann cell marker, S100. In both wild-type and T2DM

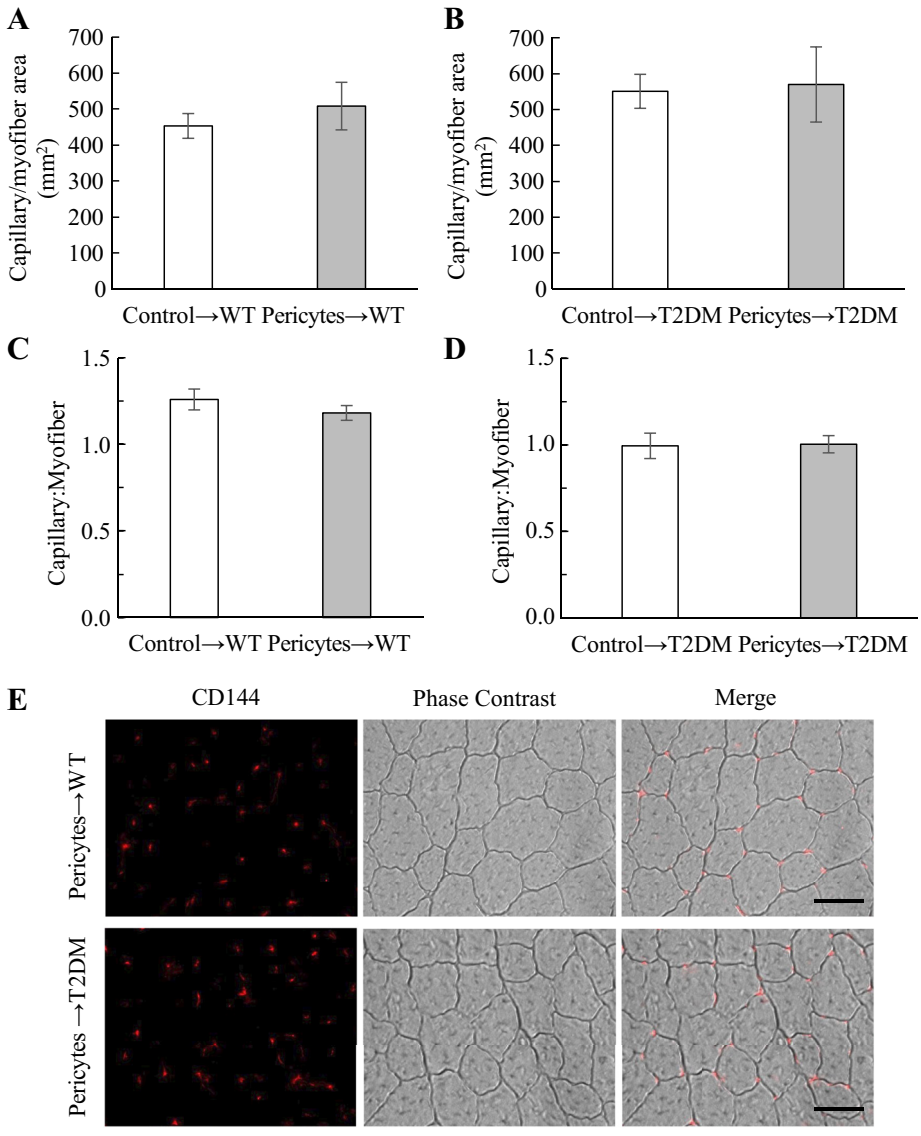

Fig. 4. Quantification of angiogenesis in wild-type (WT) and type 2 diabetes mellitus *db/db* (T2DM) ischemic mice. Angiogenesis was assessed in the gastrocnemius muscle via capillary density in wild-type mice (means ± SE, $n = 6$) (*A*) and T2DM mice (means ± SE, $n = 5$) (*B*) at POD28 following the induction of limb ischemia. Angiogenesis was also assessed via capillary-to-fiber ratio in wild-type mice (means ± SE, $n = 6$) (*C*) and T2DM mice (means ± SE, $n = 5$) (*D*) at POD28. Representative images (*E*) show CD144 immunofluorescence and phase-contrast images taken for quantification from wild-type (*top*) and T2DM (*bottom*) mice. Scale bar, 50 μm.

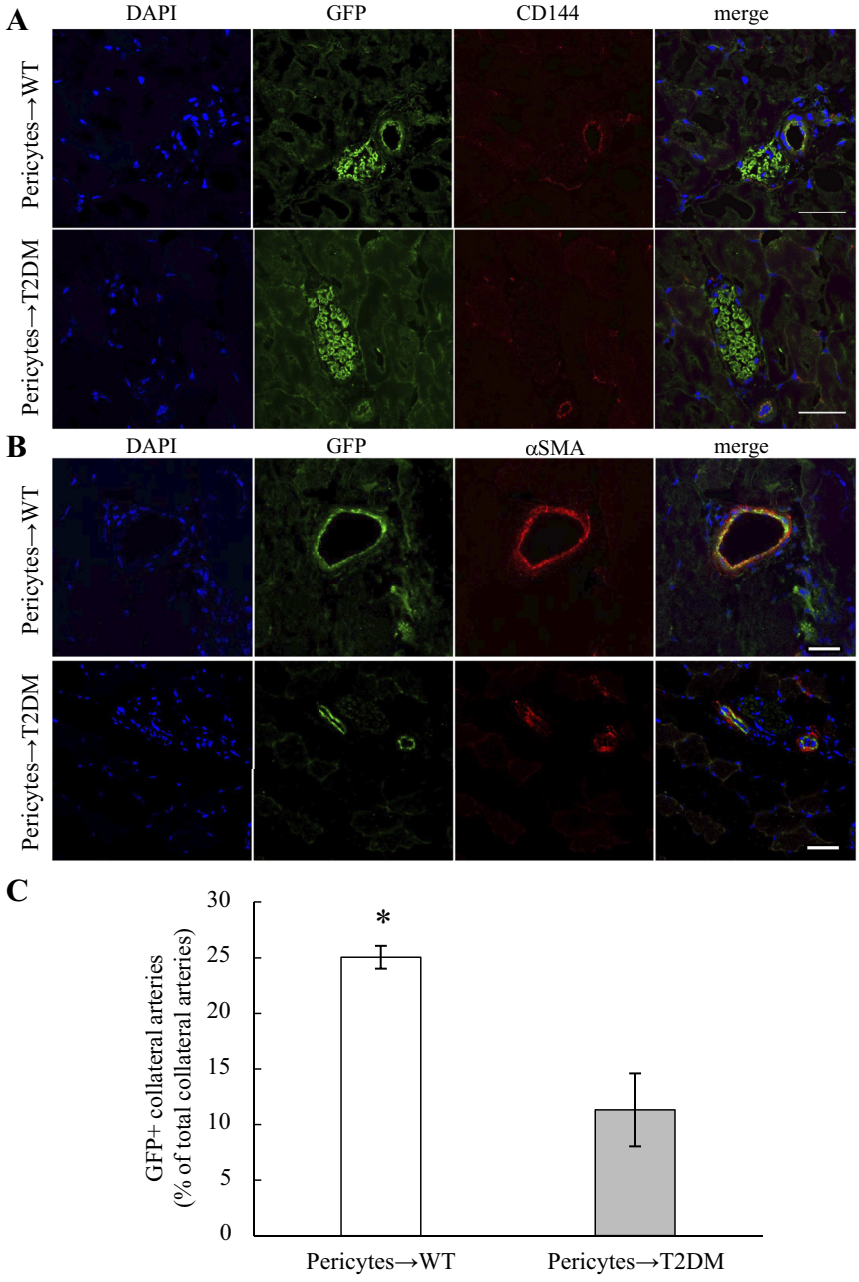

Fig. 5. In vivo engraftment of green fluorescent protein-positive (GFP^+) pericytes into collateral arteries. GFP^+ pericyte differentiation into $CD144^+$ endothelial cells was assessed in wild-type (WT; *A*, *top*) and type 2 diabetes mellitus *db/db* (T2DM) ischemic mice (*A*, *bottom*) in skeletal muscles at postoperative day 28 (POD28) following the induction of limb ischemia. GFP^+ pericyte engraftment into α-smooth muscle actin-positive (αSMA^+) collateral arteries was assessed in WT (*B*, *top*) and T2DM ischemic mice (*B*, *bottom*) in thigh muscles at POD28 following the induction of limb ischemia. Engraftment was quantified as the percentage of total αSMA^+ collateral arteries that costained positive for GFP (*C*). Scale bar, 50 μm. $^*P < 0.05$ vs. Pericytes→T2DM.

mice, costaining of GFP and S100 was observed, confirming that pericytes differentiated into Schwann cells (Fig. 6).

No GFP^+ skeletal muscle fibers were observed. Pericyte differentiation into skeletal muscle cells was not detected in gastrocnemius or thigh muscle sections of wild-type or T2DM mice.

Insulin increases oxidative stress in human primary pericytes and impairs pericyte function in vitro. Insulin significantly upregulated *Nox2* gene expression in human primary pericytes (1.74-fold vs. control; $P = 0.04$; Fig. 7*A*), and NAC treatment prevented the insulin-induced upregulation of *Nox2* gene expression. There were no differences in *Nox1* or *Nox4* gene expression between control, insulin-treated, or insulin plus NAC-treated pericytes.

Insulin impaired the ability of human primary pericytes to form tubes in vitro, which was abrogated by cotreatment with NAC. Insulin-treated pericytes formed tubes with a smaller area than control pericytes (4,052 ± 276 vs. 13,640 ± 3,687 μm^2, $P = 0.01$; Fig. 7*C*), and NAC treatment prevented the decrease in tube area that was observed in insulin treated pericytes (13,547 ± 3,029 μm^2). Insulin-treated pericytes tended to have shorter total tube lengths than control pericytes (27,817 ± 632 vs. 30,684 ± 732 μm, $P = 0.095$; Fig. 7*B*), and insulin plus NAC-treated pericytes had significantly longer total tube lengths than insulin-treated pericytes (31,822 ± 592 μm, $P = 0.048$). Overall, insulin and insulin plus NAC treatment did not affect the number of tubes formed ($P = 0.20$; Fig. 7*D*). Insulin plus NAC-treated cells had greater numbers of master junctions than insulin-treated and control pericytes (19.0 ± 0.6 vs. 10.0 ± 1.1 and 11.4 ± 1.5, respectively, $P = 0.001$ vs. control; $P < 0.001$ vs. insulin; Fig. 7*E*).

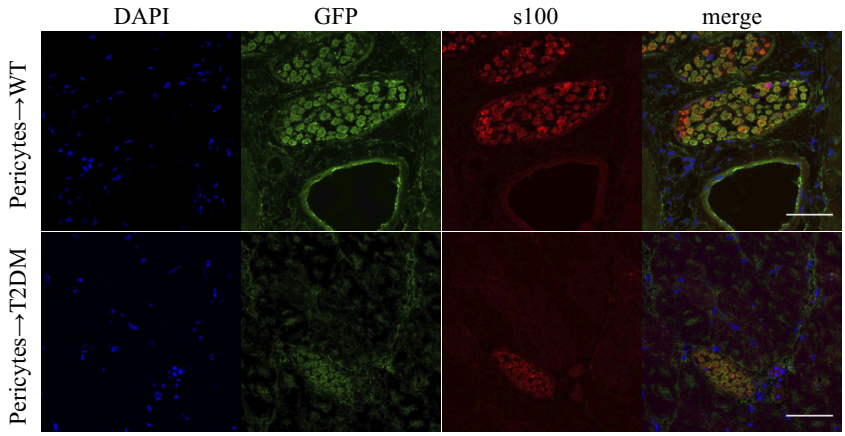

Fig. 6. In vivo differentiation of green fluorescent protein-positive (GFP^+) pericytes into Schwann cells. GFP^+ pericyte differentiation into neural cells was investigated in the skeletal muscles of wild-type (WT) and type 2 diabetes mellitus *db/db* (T2DM) ischemic mice at POD28 by examining GFP costaining with the Schwann cell marker S100. Scale bar, 50 μm.

DISCUSSION

Skeletal muscle pericytes augment postischemic neovascularization in wild-type mice, but T2DM impairs the ability of skeletal muscle pericytes to augment postischemic neovascularization, potentially via diabetes-induced oxidant stress. The most important findings of this study are: *1*) in wild-type mice, skeletal muscle pericyte cell therapy augments blood flow recovery via collateral artery enlargement, but not angiogenesis; *2*) in T2DM mice, pericyte cell therapy does not augment blood flow recovery, collateral artery enlargement, or angiogenesis; *3*) T2DM impairs pericyte engraftment into host collateral arteries in vivo; and *4*) pericytes differentiate into Schwann cells in vivo. The implications of this study are that pericyte cell therapy may be a novel treatment strategy to improve blood flow in PAD, but not for T2DM patients with PAD. Whether this impairment of pericyte function would extend to other cardiovascular risk factors remains to be seen.

A major finding of our study is that skeletal muscle pericyte cell therapy improves blood flow recovery from limb ischemia via collateral artery enlargement. In wild-type mice, pericyte cell therapy increased blood flow recovery in the ischemic limb. At 28 days after the induction of ischemia, the pericyte transplanted group recovered 17.5% more blood flow than the control transplanted group. Previous studies have also shown the therapeutic potential of skeletal muscle pericytes or similar cells to improve postischemic neovascularization in a murine limb ischemia model (3, 8, 15, 28, 30). Birbrair and colleagues (3) qualitatively showed that $Nestin^+NG2^+$ pericytes improved recovery from ischemia via incorporation into newly formed vessels 10 days after the induction of limb ischemia in athymic nude mice, but foot blood flow recovery was not quantified. In another study, pericyte-like cells derived from human pluripotent stem cells were shown to improve foot blood flow recovery via incorporation into both muscle and vasculature in immunodeficient mice (8). Gubernator and colleagues (15) transplanted saphenous vein adventitial progenitor cells, a cell type that expresses the pericyte markers NG2 and PDGFRβ, into immunodeficient mice and showed improved recovery from limb ischemia at postoperative day 28 (15). Each of these studies using pericyte-like cells supports our finding that pericytes can aid in the recovery from limb ischemia.

In our study, postischemic neovascularization was enhanced via collateral artery enlargement in the wild-type mice. Collateral artery enlargement is the main mechanism for increasing blood flow to the ischemic limbs in the murine model of limb ischemia (23). To our knowledge, only one study has used the murine limb ischemia model to examine the role of pericytes to augment postischemic neovascularization via collateral artery enlargement. Birbrair and colleagues (3) used in vivo MRI angiography to qualitatively show collateral remodeling in the ischemic hindlimbs of mice following pericyte cell transplantation.

Blood flow recovery can also be augmented via angiogenesis; however, pericyte cell therapy did not improve angiogenesis in our study, as assessed by capillary-to-fiber ratio and capillary density. In contrast to the findings of this study, Dar et al. (8) observed increased blood vessel density in ischemic limbs transplanted with pericytes than in nontransplanted controls. There are limited studies that examine the effect of pericyte transplantation on angiogenesis during postischemic neovascularization, but MSCs have been shown to improve angiogenesis during postischemic neovascularization in wild-type mice (30). It is unknown why pericyte transplantation did not significantly improve angiogenesis in this study, but may represent an important difference between mechanisms of blood flow recovery between skeletal muscle pericytes and similar cell types, such as MSCs.

Stem cell therapies are known to be less effective due to diabetes (12, 30), but preclinical models often fail to test the efficacy of stem cell therapies in animals with comorbidities. A strength of our study is that the efficacy of a pericyte cell therapy was tested in a clinically relevant T2DM model of PAD. We found that the T2DM environment impairs the ability of skeletal muscle pericytes to improve blood flow recovery, collateral artery enlargement, or angiogenesis following the induction of limb ischemia. Yan et al. (30) tested the efficacy of an MSC therapy to augment postischemic neovascularization in immunocompetent wild-type and T2DM mice. They found that although MSCs could augment postischemic neovascularization in wild-type mice by 15% ($79 \pm 2\%$ vs. $64 \pm 1\%$ in controls), diabetes impaired the ability of MSCs to augment postischemic neovascularization.

The mechanisms by which the type 2 diabetic environment impairs pericyte cell therapy were not examined in vivo in our study. However, our in vitro evidence indicates that T2DM increases pericyte oxidant stress, which negatively affects the function of pericytes. We showed that insulin treatment in

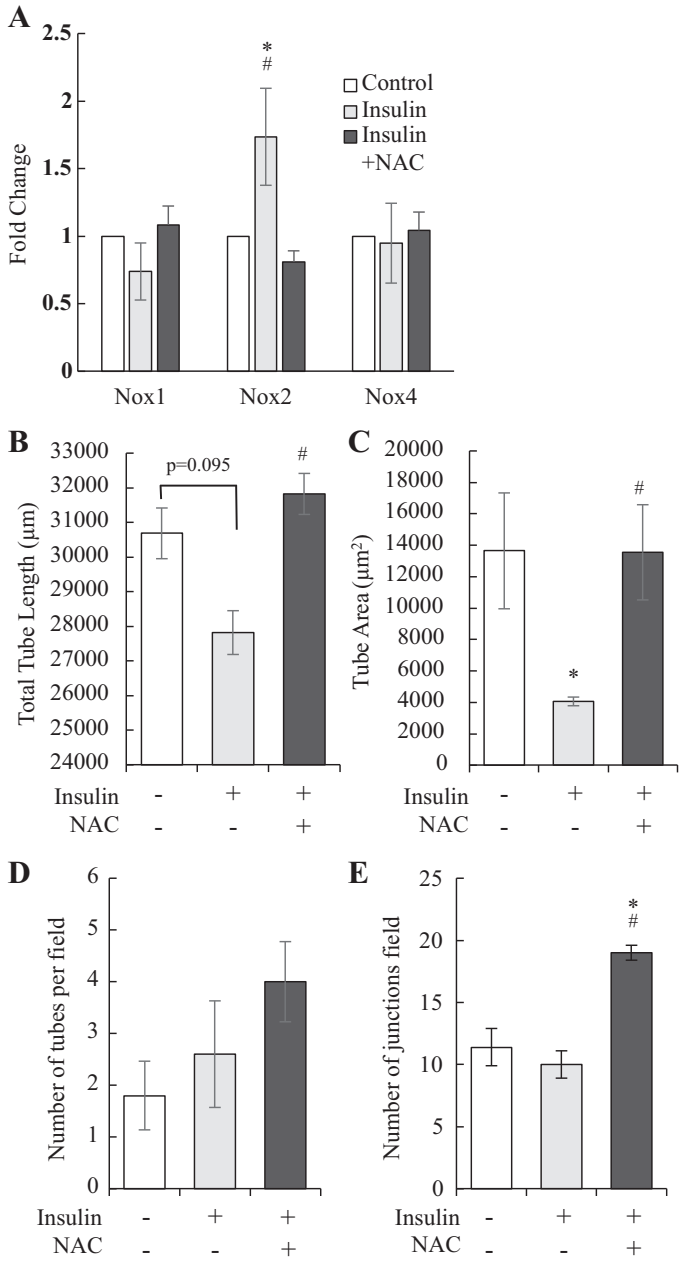

Fig. 7. Effect of insulin and *N*-acetylcysteine (NAC) on pericyte gene expression and tube formation in vitro. The expression of NADPH oxidase genes was assessed in human primary pericytes treated with insulin or insulin plus NAC (*A*). Tube formation of human primary pericytes treated with insulin or insulin plus NAC was quantified via total tube length (*B*), average tube area (*C*), number of tubes formed per microscopic field (*D*), and the number of master junctions per microscopic field (*E*). *$P < 0.05$ vs. untreated Control; #$P < 0.05$ vs. Insulin.

human primary pericytes, which mimics the hyperinsulinemia that is common in T2DM, induces an upregulation of the NADPH oxidase gene *Nox2*, and that treatment with the antioxidant NAC prevents *Nox2* upregulation. We utilized a tube formation assay in vitro to show that insulin treatment impairs pericyte tube formation capacity. Further, we showed that treatment with NAC prevents insulin from impairing pericyte tube formation. We also demonstrated that NAC treatment increased the complexity of tubular networks in our study. In support of these findings, an investigation of human skeletal muscle pericytes from diabetic patients with critical limb ischemia showed that pericytes from diabetic donors had increased oxidant stress compared with pericytes from donors without diabetes (28). Further, Yan et al. (30) showed that oxidant stress is the mechanism by which T2DM negatively impacts stem cell therapy in mice. Together, these findings indicate that oxidant stress may be the underlying mechanism by which type 2 diabetes impairs pericyte cell therapy in our study.

Another major finding of our study is that pericytes can differentiate in vivo during postischemic neovascularization in wild-type and T2DM mice. We observed that transplanted pericytes engraft into collateral arteries in the thigh muscles. Engraftment into collateral arteries was confirmed in both wild-type and T2DM mice, but T2DM impaired the incorporation of skeletal muscle pericytes into collateral arteries in vivo. Pericyte engraftment into collateral arteries may be one mechanism by which pericytes improve collateral artery enlargement and augment blood flow recovery in wild-type, but not T2DM mice following the induction of limb ischemia. In support of our findings, previous studies showed that T2DM negatively affects stem cell differentiation (28, 30). Yan et al. (30) showed that T2DM impaired the in vivo differentiation capacity of transplanted MSCs in mice by skewing differentiation away from endothelial cells and toward adipocytes following the induction of limb ischemia (30). In humans, pericytes isolated from the skeletal muscles of diabetic patients had skewed in vitro differentiation toward adipocytes (28). Adipogenic differentiation of pericytes was not investigated in the current study, nor was it informally observed.

Next, we found that collateral arteries that were positive for pericyte incorporation were often observed near GFP+ structures that were identified as Schwann cells, indicating that pericytes differentiated into Schwann cells. Schwann cells are glial cells of the peripheral nervous system that support axons and are involved in nerve repair and myelination (17). Previous studies have shown that pericyte-like cells from the central nervous system can be induced to express glial markers in vitro (10). Further, a population of nestin$^+$ skeletal muscle neural precursors were identified by Birbrair and colleagues (2) and shown to possess gliogenic potential, thus demonstrating the possibility of skeletal muscle resident pericytes to contribute to peripheral nervous system glial cells in vivo. Differentiation of skeletal muscle pericytes toward glial cells during postischemic neovascularization may be an important component of overall tissue recovery. Interestingly, differentiation into Schwann cells was observed in both wild-type and T2DM mice. Peripheral neuropathy is a negative consequence of T2DM. Schwann cell dysfunction has been implicated in the pathogenesis of diabetic neuropathy (11). A cell therapy that is designed to increase blood flow while also treating neuropathy would be beneficial to diabetic patients with PAD and warrants further investigation into the mechanism of pericyte gliogenic differentiation in vivo.

There was no indication of pericyte differentiation into skeletal myocytes in vivo in wild-type or T2DM mice despite evidence for in vitro pericyte myogenic differentiation in our study. Previous studies have shown that pericyte-like cells can differentiate into skeletal muscle (8), but that was not observed in this study. Reasons for the lack of myogenic differentiation

could include differences in the number or type of transplanted cells. For example, Dar et al. (8) transplanted 2×10^6 human-induced pluripotent stem cells into immunodeficient mice following the induction of limb ischemia and observed myogenic differentiation, whereas 1×10^5 skeletal muscle pericytes were transplanted into immunocompetent hosts in this study. There could be several reasons why skeletal myogenic differentiation was not detected after transplantation of 1×10^5 pericytes. First, myogenic differentiation may not have occurred in this model. Second, myogenic differentiation may have occurred infrequently, but was not observed in the skeletal muscle sections that were examined. Finally, perhaps pericytes fused with existing multinucleated muscle fibers, but the GFP signal was too weak to detect.

The current study has limitations. First, our study utilized an acute PAD model in young mice. PAD is a progressive disease that is often seen in the aging population; therefore, using an aged mouse model and a progressive ischemia model would increase the clinical relevance. Second, the study is limited because it examines the negative impact of the diabetic environment on the ability of pericytes to augment postischemic neovascularization, but it does not examine the ability of pericytes from diabetic mice to augment postischemic neovascularization. Autologous stem cell transplantations are a goal of clinical PAD therapies; and therefore, the ability of a diabetic pericyte transplantation to enhance neovascularization should be investigated in future studies.

In summary, skeletal muscle pericytes augment postischemic neovascularization in wild-type mice, but T2DM impairs the ability of skeletal muscle pericytes to augment postischemic neovascularization. Following the induction of limb ischemia, pericyte transplantation improves collateral artery enlargement in wild-type mice, but not in T2DM mice. Further, pericytes incorporate into collateral arteries at a greater rate in wild-type mice than in T2DM mice, and in vivo differentiation into Schwann cells occurs in both wild-type and T2DM mice. Pericytes are a novel cell type that may be beneficial for the treatment of diabetic PAD. However, future studies are needed to examine ways to overcome the diabetic impairment, potentially through the use of antioxidants, to improve the efficacy of pericyte cell therapy for diabetic patients with PAD.

ACKNOWLEDGMENTS

The authors thank Dr. Lyne Khair at the University of Massachusetts (UMass) Medical School for help with data collection and Dr. James Chambers for assistance with generating the microscopy data in the Light Microscopy Facility and Nikon Center of Excellence at the Institute for Applied Life Sciences, UMass Amherst, with support from the Massachusetts Life Sciences Center.

Present address of S. Witkowski: Department of Exercise and Sport Studies, Smith College, Northampton, MA 01063.

GRANTS

This work was supported by National Heart, Lung, and Blood Institute Grant 5R01HL124101-04 (to L. M. Messina). K. L. Hayes was funded by an American Dissertation Fellowship from the American Association of University Women. L. M. Schwartz is supported by a Eugene M. and Ronnie Isenberg Professorship Endowment.

DISCLOSURES

No conflicts of interest, financial or otherwise, are declared by the authors.

AUTHOR CONTRIBUTIONS

K.L.H., L.M.M., and S.W. conceived and designed research; K.L.H. and A.S.B. performed experiments; K.L.H. analyzed data; K.L.H., L.M.M., L.M.S., J.Y., and S.W. interpreted results of experiments; K.L.H. prepared figures; K.L.H. drafted manuscript; K.L.H., L.M.M., L.M.S., J.Y., and S.W. edited and revised manuscript; K.L.H., L.M.M., L.M.S., J.Y., A.S.B., and S.W. approved final version of manuscript.

REFERENCES

1. **Armulik A, Abramsson A, Betsholtz C.** Endothelial/pericyte interactions. *Circ Res* 97: 512–523, 2005. doi:10.1161/01.RES.0000182903.16652.d7.
2. **Birbrair A, Wang ZM, Messi ML, Enikolopov GN, Delbono O.** Nestin-GFP transgene reveals neural precursor cells in adult skeletal muscle. *PLoS One* 6: e16816, 2011. doi:10.1371/journal.pone.0016816.
3. **Birbrair A, Zhang T, Wang ZM, Messi ML, Olson JD, Mintz A, Delbono O.** Type-2 pericytes participate in normal and tumoral angiogenesis. *Am J Physiol Cell Physiol* 307: C25–C38, 2014. doi:10.1152/ajpcell.00084.2014.
4. **Cappellari O, Cossu G.** Pericytes in development and pathology of skeletal muscle. *Circ Res* 113: 341–347, 2013. doi:10.1161/CIRCRESAHA.113.300203.
5. **Chen WC, Baily JE, Corselli M, Díaz ME, Sun B, Xiang G, Gray GA, Huard J, Péault B.** Human myocardial pericytes: multipotent mesodermal precursors exhibiting cardiac specificity. *Stem Cells* 33: 557–573, 2015. doi:10.1002/stem.1868.
6. **Chen WC, Saparov A, Corselli M, Crisan M, Zheng B, Péault B, Huard J.** Isolation of blood-vessel-derived multipotent precursors from human skeletal muscle. *J Vis Exp* 90: e51195, 2014. doi:10.3791/51195.
7. **Corselli M, Crisan M, Murray IR, West CC, Scholes J, Codrea F, Khan N, Péault B.** Identification of perivascular mesenchymal stromal/stem cells by flow cytometry. *Cytometry A* 83: 714–720, 2013. doi:10.1002/cyto.a.22313.
8. **Dar A, Domev H, Ben-Yosef O, Tzukerman M, Zeevi-Levin N, Novak A, Germanguz I, Amit M, Itskovitz-Eldor J.** Multipotent vasculogenic pericytes from human pluripotent stem cells promote recovery of murine ischemic limb. *Circulation* 125: 87–99, 2012. doi:10.1161/CIRCULATIONAHA.111.048264.
9. **Dellavalle A, Maroli G, Covarello D, Azzoni E, Innocenzi A, Perani L, Antonini S, Sambasivan R, Brunelli S, Tajbakhsh S, Cossu G.** Pericytes resident in postnatal skeletal muscle differentiate into muscle fibres and generate satellite cells. *Nat Commun* 2: 499, 2011. doi:10.1038/ncomms1508.
10. **Dore-Duffy P, Katychev A, Wang X, Van Buren E.** CNS microvascular pericytes exhibit multipotential stem cell activity. *J Cereb Blood Flow Metab* 26: 613–624, 2006. doi:10.1038/sj.jcbfm.9600272.
11. **Eckersley L.** Role of the Schwann cell in diabetic neuropathy. *Int Rev Neurobiol* 50: 293–321, 2002. doi:10.1016/S0074-7742(02)50081-7.
12. **Efimenko AY, Kochegura TN, Akopyan ZA, Parfyonova YV.** Autologous stem cell therapy: how aging and chronic diseases affect stem and progenitor cells. *Biores Open Access* 4: 26–38, 2015. doi:10.1089/biores.2014.0042.
13. **Fowkes FG, Rudan D, Rudan I, Aboyans V, Denenberg JO, McDermott MM, Norman PE, Sampson UK, Williams LJ, Mensah GA, Criqui MH.** Comparison of global estimates of prevalence and risk factors for peripheral artery disease in 2000 and 2010: a systematic review and analysis. *Lancet* 382: 1329–1340, 2013. doi:10.1016/S0140-6736(13)61249-0.
14. **Geevarghese A, Herman IM.** Pericyte-endothelial crosstalk: implications and opportunities for advanced cellular therapies. *Transl Res* 163: 296–306, 2014. doi:10.1016/j.trsl.2014.01.011.
15. **Gubernator M, Slater SC, Spencer HL, Spiteri I, Sottoriva A, Riu F, Rowlinson J, Avolio E, Katare R, Mangialardi G, Oikawa A, Reni C, Campagnolo P, Spinetti G, Touloumis A, Tavaré S, Prandi F, Pesce M, Hofner M, Klemens V, Emanueli C, Angelini G, Madeddu P.** Epigenetic profile of human adventitial progenitor cells correlates with therapeutic outcomes in a mouse model of limb ischemia. *Arterioscler Thromb Vasc Biol* 35: 675–688, 2015. doi:10.1161/ATVBAHA.114.304989.
16. **Kabara M, Kawabe J, Matsuki M, Hira Y, Minoshima A, Shimamura K, Yamauchi A, Aonuma T, Nishimura M, Saito Y, Takehara N, Hasebe N.** Immortalized multipotent pericytes derived from the vasa vasorum in the injured vasculature. A cellular tool for studies of vascular

remodeling and regeneration. *Lab Invest* 94: 1340–1354, 2014. doi:10.1038/labinvest.2014.121.

17. **Kim HA, Mindos T, Parkinson DB.** Plastic fantastic: Schwann cells and repair of the peripheral nervous system. *Stem Cells Transl Med* 2: 553–557, 2013. doi:10.5966/sctm.2013-0011.
18. **Limbourg A, Korff T, Napp LC, Schaper W, Drexler H, Limbourg FP.** Evaluation of postnatal arteriogenesis and angiogenesis in a mouse model of hind-limb ischemia. *Nat Protoc* 4: 1737–1748, 2009. doi:10.1038/nprot.2009.185.
19. **Lotfi S, Patel AS, Mattock K, Egginton S, Smith A, Modarai B.** Towards a more relevant hind limb model of muscle ischaemia. *Atherosclerosis* 227: 1–8, 2013. doi:10.1016/j.atherosclerosis.2012.10.060.
20. **Pfaffl MW, Tichopad A, Prgomet C, Neuvians TP.** Determination of stable housekeeping genes, differentially regulated target genes and sample integrity: *BestKeeper*–Excel-based tool using pair-wise correlations. *Biotechnol Lett* 26: 509–515, 2004. doi:10.1023/B:BILE.0000019559.84305.47.
21. **Sacchetti B, Funari A, Remoli C, Giannicola G, Kogler G, Liedtke S, Cossu G, Serafini M, Sampaolesi M, Tagliafico E, Tenedini E, Saggio I, Robey PG, Riminucci M, Bianco P.** No identical "mesenchymal stem cells" at different times and sites: human committed progenitors of distinct origin and differentiation potential are incorporated as adventitial cells in microvessels. *Stem Cell Reports* 6: 897–913, 2016. doi:10.1016/j.stemcr.2016.05.011.
22. **Sampson UK, Fowkes FG, McDermott MM, Criqui MH, Aboyans V, Norman PE, Forouzanfar MH, Naghavi M, Song Y, Harrell FE Jr, Denenberg JO, Mensah GA, Ezzati M, Murray C.** Global and regional burden of death and disability from peripheral artery disease: 21 world regions, 1990 to 2010. *Glob Heart* 9: 145–158.e21, 2014. doi:10.1016/j.gheart.2013.12.008.
23. **Scholz D, Ziegelhoeffer T, Helisch A, Wagner S, Friedrich C, Podzuweit T, Schaper W.** Contribution of arteriogenesis and angiogenesis to postocclusive hindlimb perfusion in mice. *J Mol Cell Cardiol* 34: 775–787, 2002. doi:10.1006/jmcc.2002.2013.
24. **Stapor PC, Sweat RS, Dashti DC, Betancourt AM, Murfee WL.** Pericyte dynamics during angiogenesis: new insights from new identities. *J Vasc Res* 51: 163–174, 2014. doi:10.1159/000362276.
25. **Tang G, Charo DN, Wang R, Charo IF, Messina L.** CCR2$^{-/-}$ knockout mice revascularize normally in response to severe hindlimb ischemia. *J Vasc Surg* 40: 786–795, 2004. doi:10.1016/j.jvs.2004.07.012.
26. **Tang GL, Chang DS, Sarkar R, Wang R, Messina LM.** The effect of gradual or acute arterial occlusion on skeletal muscle blood flow, arteriogenesis, and inflammation in rat hindlimb ischemia. *J Vasc Surg* 41: 312–320, 2005. doi:10.1016/j.jvs.2004.11.012.
27. **Thiruvoipati T, Kielhorn CE, Armstrong EJ.** Peripheral artery disease in patients with diabetes: Epidemiology, mechanisms, and outcomes. *World J Diabetes* 6: 961–969, 2015. doi:10.4239/wjd.v6.i7.961.
28. **Vono R, Fuoco C, Testa S, Pirrò S, Maselli D, Ferland McCollough D, Sangalli E, Pintus G, Giordo R, Finzi G, Sessa F, Cardani R, Gotti A, Losa S, Cesareni G, Rizzi R, Bearzi C, Cannata S, Spinetti G, Gargioli C, Madeddu P.** Activation of the pro-oxidant PKCβII-p66^{Shc} signaling pathway contributes to pericyte dysfunction in skeletal muscles of patients with diabetes with critical limb ischemia. *Diabetes* 65: 3691–3704, 2016. doi:10.2337/db16-0248.
29. **Yan J, Tie G, Park B, Yan Y, Nowicki PT, Messina LM.** Recovery from hind limb ischemia is less effective in type 2 than in type 1 diabetic mice: roles of endothelial nitric oxide synthase and endothelial progenitor cells. *J Vasc Surg* 50: 1412–1422, 2009. doi:10.1016/j.jvs.2009.08.007.
30. **Yan J, Tie G, Wang S, Messina KE, DiDato S, Guo S, Messina LM.** Type 2 diabetes restricts multipotency of mesenchymal stem cells and impairs their capacity to augment postischemic neovascularization in db/db mice. *J Am Heart Assoc* 1: e002238, 2012. doi:10.1161/JAHA.112.002238.